Celal Bayar University Journal of Science

Comparative Investigation of Edge Cracking Behavior in 600 MPa Dual Phase (DU) Steel Sheets from Different Manufacturers

Zeki Ahmet Ekmen[1]*, Yiğit Gönülalan[2], Onur Muratal[3], Diğdem Atabek[4]

[1,2,3,4] TOYOTETSU Otomotiv Parçaları San. ve Tic. A.Ş., Kocaeli, Türkiye
* ahmetekmen33@gmail.com.tr
* Orcid No: 0009-0009-0369-5024

Received: January 8, 2025
Accepted: May 12, 2025
DOI: 10.18466/cbayarfbe.1614992

Abstract

Recent advancements in the automotive industry have emphasized the importance of fuel efficiency, weight reduction, and durability. In response, AHSS materials have become widely used, particularly in cold forming. However, their high strength reduces formability, leading to challenges such as edge cracking. In this study, 600DU steel from two different mills was tested. Tensile tests were conducted on EU1 and EU2 at 0°, 45°, and 90° to the rolling direction per JIS Z 2241 No. 5. The tensile strength values were similar, but EU2 showed higher elongation. A hole expansion test revealed an average expansion of ~27% for EU1 and ~60% for EU2. Vickers hardness was measured under an HV 10 load. Metallographic preparation was followed by microstructural analysis using optical and SEM microscopy. In the AutoForm simulation analysis, the average thickness reduction of the EU1 steel was determined to be 19%, while that of the EU2 steel was measured at 11%. These results indicate that the EU1 steel exhibits 8% greater thinning compared to the EU2 steel. This study examines the formability of 600DU (dual-phase) AHSS steel from different manufacturers using numerical and experimental methods. The findings provide key insights into AHSS forming performance and help address potential issues. Numerical and experimental data modeling will contribute to optimizing manufacturing processes.

Keywords: Advanced High-Strength, Steel (AHSS), Dual-Phase Steel, Cold Forming, Formability, Numerical and Experimental Methods.

1. Introduction

Recently, lightweight components have garnered significant attention due to their influence to enhance fuel efficiency and reduce emissions [1]. Numerous aspects influence and guide the selection of materials for automotive applications, including safety, fuel efficiency, environmental impact, manufacturability, durability, and overall quality [2]. In response to these demands, novel materials with high strength-to-weight ratios, such as AHSS, are being increasingly elevated [3-4]. Among these, AHSS, especially DU steels, are extensively utilized in automotive body structures that require superior strength [5]. Recent breakthroughs in the steel industry have led to the development of DU steels that may attain a tensile strength up to 1200 MPa, reasonable elongation around 10 to 15% [6]. AHSS materials are categorized into three generations: 1st Generation (DU steels), which are characterized by favorable weldability and cost-effectiveness, making them particularly suitable for automotive applications. [7].

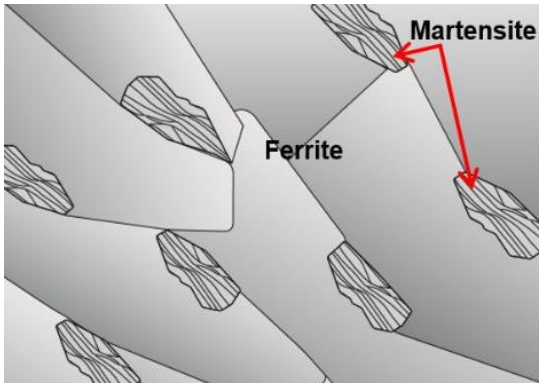

Figure 1. Schematic of a Dual Phase steel microstructure showing islands of martensite in a matrix of ferrite [8].

The steel composition includes 0.05–0.2% carbon, 1.2–1.6% manganese, 0.03–0.6% silicon, and microalloying elements, this microstructure permits tensile strengths between 500 to 1200 MPa. However, this steel exhibits low yield elongation and restricted plastic strain capacity, making it unsuitable for high-tensile applications [3]. The ferritic and martensitic microstructures affect dislocation storage and internal stresses due to differing stress-strain responses between phases [9]. Increased ferrite content enhances ductility, improving formability [10]. As illustrated in Figure 1, DU steels consist of a predominantly soft ferritic matrix, interspersed with hard martensitic phases. [11]. This study investigates the quality and performance differences of steels from two manufacturers, focusing on mechanical and physical qualities and their impact on performance. The deformation incompatibility between the martensite and ferrite phases in DU steels facilitates microcrack formation, but localized deformation in ferrite can mitigate brittle fracture. Standard techniques for damage evolution, such as analyzing void volume fraction after deformation, are crucial for failure prediction [12]. Microstructural variations considerably affect forming performance, essential in bending and tensile processes [13]. Dual-phase steels also quantity residual austenite, and the ferrite phase's internal tensile stresses contribute to lower yield strength [14]. Figure 2 illustrates the martensite fraction strongly influences tensile strength, with higher martensite content and carbon content improving tensile strength.

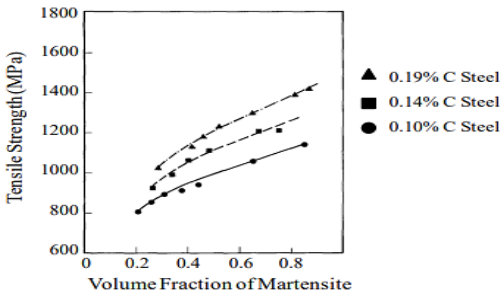

Figure 2. Tensile strength versus martensite fraction of a DU steel in different C contents [15].

Research has investigated that as the martensite volume fraction increases, tensile strength rises, but ductility associated with cracking diminishes [16]. The forming process of complex components typically involves multi-phase operations such as cutting, press forming, hole punching, and hole flanging. Steel sheet forming capabilities include deep drawing, bulging, bending, and stretch-flanging, with stretch-flanging being crucial to prevent cracking during the shaping of components. [17]. Broberg categorized the energy regions at the crack tip into the FPZ (fracture process zone) and the outer plastic zone, with the FPZ being independent of stress or loading conditions, while the outer plastic zone depends on stress state, crack length, and geometry [18]. The sheared edge consists of four zones (Figure 3): roll-over, burnish, fractured, and burr zones, with a secondary burnish zone possible depending on material properties and constraints applied to the blank [19]. Edge extension correction in DU steels is vital due to significant edge crack occurrence during cold forming. While numerical simulations provide safety margins, unexpected cracks may still occur. Edge cracks can arise from high deformation, limited edge extension capability, and poor cut edges [20]. Operations like blanking, edge trimming, and punching can create surface irregularities, reducing forming potential in the SAZ (shear-affected zone), which lowers ductility and increases premature edge cracking, especially in DU steels [21]. Factors such as work hardening, residual stress, surface roughness, and voids influence edge ductility, with cutting parameters like gap, angle, speed, and tool sharpness significantly affecting edge performance during forming [22].

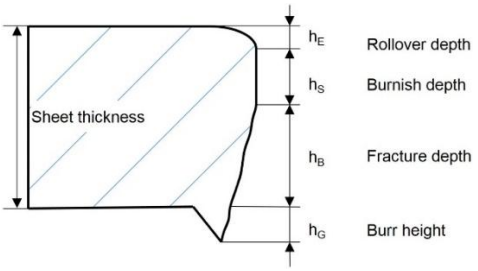

Figure 3. Schematic of the shear cutting process and SAZ containing rollover, burnish, fracture, and burr regions [23].

Golovashchenko, Zhou and colleagues proposed that sheared edge stretchability, measured in diffuse necking area and in hole expansion test illustrated that the best stretchability can be achieved for the shearing clearances 10-15% of the thickness. [24].

Clearance c refers to the distance between the punch and the die opening, such that:

$$c = \frac{D_m - d_p}{2} \tag{1}$$

The theoretical approach articulates clearance as a function of material thickness and shear strength. That is:

$$c = \frac{k.T.\sqrt{\tau_m}}{2} = \frac{k.T.\sqrt{0.7UTS}}{2} \; for\; T \leq 3\; mm \tag{2}$$

$$c = \frac{(1.5.k.T - 0{,}0015).\sqrt{0.7UTS}}{2} \; for\; T > 3\; mm \tag{3}$$

Where:

T= thickness of material (mm)
K= a coefficient that depends on the type of die; that is k=0,005 to 0,035, most frequently uses k=0.01.
τ_m = shear strength of material

UTS= Ultimate Tensile Strength [25]. This formula was used when calculating the die clearance.
This investigation examines the quality variations and performance characteristics of 600DU steel obtained from two different manufacturers, with a specific focus on preventing edge cracking and splitting in cold forming processes. To achieve this objective, the mechanical and physical properties of 600DU steel from different manufacturers are experimentally evaluated to determine their influence on the formation of edge defects during forming operations. Additionally, this study seeks to numerically compare the edge cracking behavior of these steels through simulations conducted using AutoForm software, identifying critical deformation zones and assessing their impact on formability. The findings of this research are expected to provide scientific insights for optimizing material selection in high-strength steel applications, particularly in the automotive and manufacturing industries.

Materials and Methods

2.1. Materials

The experimental study focused on steel coils of identical strength and size obtained from various manufacturers, designated as EU1 and EU2. The production of 600DU steels is carried out in accordance with specific standard values, and the supplied products were procured from manufacturers that comply with the requirements of the JIS: G 3141 standard. The materials used were classified as 600DU, with dimensions maintained as in mass production, and no modifications were made to the press and die setup. The chemical compositions of the 600DU steel coils obtained from EU1 and EU2 are presented in Table 1, which constitute fundamental elements influencing the mechanical and physical properties of the material. Chemical composition is crucial for production processes and product quality, and the analysis of the data presented in Table 1 is essential for understanding the characteristics and applications of 600DU steel.

Table 1. Chemical Percentage Values of Steels

	Chemical Proporties						
Steel Grade	C (%)	Si (%)	Cr (%)	Mn (%)	Al (%)	P (%)	S (%)
EU1	≤0,15	≤0,80	≤1	≤2,50	0,015-1,0	≤0,05	≤0,010
EU2	≤0,15	≤0,75	≤1	≤2,50	0,015-1,0	≤0,040	≤0,010

2.2. Experimental and Numerical Testing Methods

2.2.1. Preparation of Microstructural Specimens

In the investigation, EU1 and EU2 materials were prepared metallographically and then characterized microstructurally. The specimens were prepared metallographically on a Struers brand Tegramin 25 model automatic grinding-polishing device. Final polishing was completed using Dia Pro Nap B 1 µm solution on an MD Nap disk. Specimen preparation processes were applied in accordance with ASTM E3 standards. After metallographic processes, chemical etching was applied to the specimens with 2% nital solution. After the etching process, microstructural images were obtained using a Nikon brand ECLIPSE MA 100 model optical microscope and quantitative metallographic software (Clemex Vision Lite, Image Analysis Software 2.0C). SEM (scanning electron microscope) images of the specimens were obtained on a ZEISS brand EVO 10 model device.

2.2.2. Preparation of Specimens for Tensile and Hardness Testing

Following the microstructural characterization of the specimens, the Vickers hardness test was conducted under an HV10 load in accordance with TS EN ISO 6507-1 standards. The Vickers hardness test was conducted on EMCOTEST brand Durascan 20 G5 model device. The tensile test was carried out using an Instron 5985 model tensile testing machine. The test was performed with a grip displacement speed of 0.00025 mm/s up to the yield point and 0.0067 mm/s after the yield point. The test was conducted in accordance with the JIS Z 2241 standard. For verification purposes, three tensile test specimens of EU1 and EU2 materials from each angle (Figure 4) were obtained at 0°, 45°, and 90° angles to the rolling directions using the tensile test specimen cutting die shown in Figure 4b. The tensile tests were carried out in accordance with the JIS Z 2241 standard.

Celal Bayar University Journal of Science
Volume 21, Issue 3, 2025, p 10-20
Doi: 10.18466/cbayarfbe.1614992

In order to determine the % elongation values, the AVE 2 Non-Contacting Video Extensometer device was used. The gauge length was specified as L0=50 mm according to the JIS Z 2241 standard.

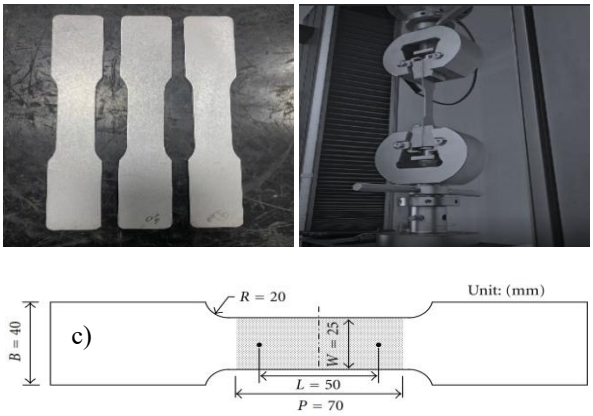

Figure 4. Tensile Tests L_o=50mm a) Specimens,b) Machine of Tention Specimens c) JIS Z 2241 No. 5 specimen

2.2.3. Preparation of Test Specimens for Hole Expansion Ratio

This study seeks to compare cracks occurring during the edge forming process in cold forming operations, considering different materials and forming parameters. Experimental investigations were conducted to identify factors influencing crack formation and determine optimal process parameters. Stretch-flangeability, which indicates edge formability, was assessed using the HER (hole expansion ratio) test [26]. The specimen preparation involved cutting the material into 100 mm x 100 mm (Figure 5) pieces, followed by hole drilling in the HER die to ensure proper centering. A hole matrix of 10.30 mm (Figure 5) was selected for the 1.4 mm thick specimens. The Hole Expansion device (Figure 5), comprising hydraulic, mechanical, and camera units, was used for testing. Specimens were aligned with the rolling direction and positioned with the cutting surface facing the conical punch to ensure reliable and repeatable results.

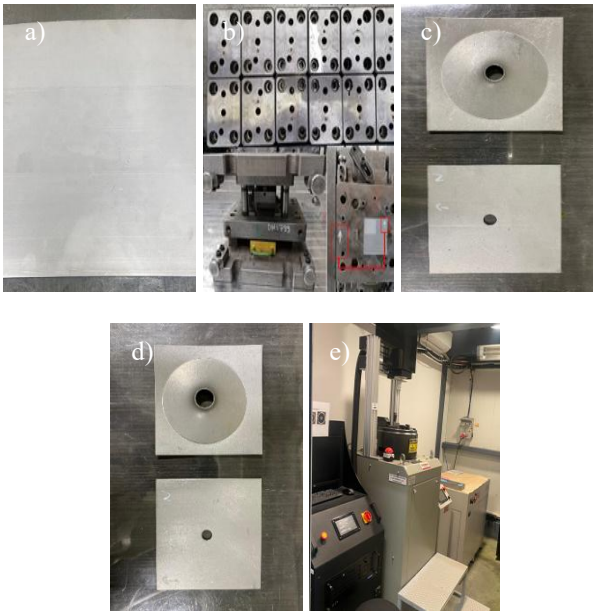

Figure 5. a) Big Sheet Material, b) Die of hole Expansion Specimen Die, c) Specimen of EU1 Company, d) Specimen of EU1, e)Hole Expansion Test Device

2.3. Forming Simulation

AutoForm software is a specialized tool designed for the simulation and optimization of sheet metal forming processes. This software aids in enhancing production efficiency by virtually modeling various processes such as cutting, bending, and cam pierce. In this study, a case study involving a fender apron wind guige part was selected. The dimensions and material properties of the 600DU steel were defined, and the die geometry was created using Catia software. This geometry was then transferred to the AutoForm R8 program, where material cards (Figure 6 and Figure 7) for EU1 and EU2 steels were defined. Appropriate process steps were established, and the simulation was executed with adjusted parameters to predict the effects of edge cracking on the final part formation, considering the properties of EU1 and EU2 materials.

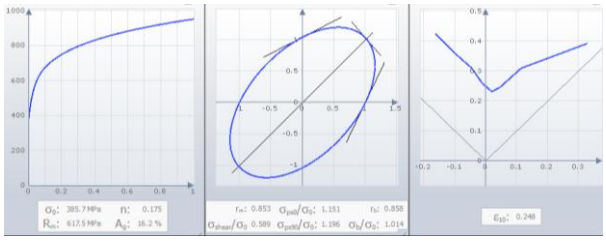

Figure 6. Selection Material Card of EU1

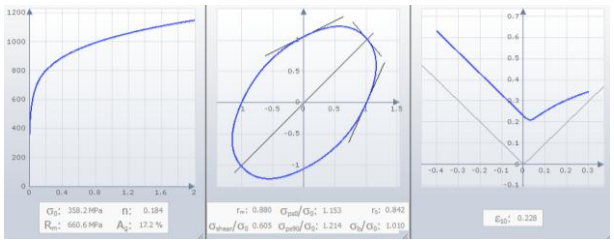

Figure 7. Selection Material Card of EU2

2.4. Die Trial Flow

In this experiment, the die clearance was calculated based on the parameters outlined in Equation 2, resulting in a value of 12.5%. This clearance played a crucial role in ensuring optimal material flow and minimizing issues such as edge cracking during the forming process. The experimental procedure involved nine distinct operations aimed at assessing the material's formability and performance. These operations included forming, cutting, bending, and cam piercing, all performed sequentially to simulate cold forming conditions. The trials were conducted using a 1200-ton eccentric press, providing sufficient force for the various forming operations required in this study. The use of such high-tonnage equipment allowed the simulation of realistic press forming conditions, closely resembling those encountered in industrial applications. Each stage of the trial provided valuable insights into the material's behavior under different loading conditions and its susceptibility to defects such as thinning or cracking.

3. Results and Discussion

3.1. Microstructural Characterization

Figure 8 illustrates the optical microstructures of 600DU material from two distinct manufacturers. The martensitic phase, visible as dark contrast regions, is primarily located at the grain boundaries of the lighter contrast ferritic phase [27]. The martensite band structure is also significant. Damage initiation is significantly influenced by microstructural characteristics and strain heterogeneity, with factors such as grain size and martensite volume fraction being critical in determining material response to loading. The morphology of the martensite phase plays a key role in early-stage damage nucleation, with banded martensitic structures being more prone to cracking compared to ferrite-martensite interface decohesion [28].

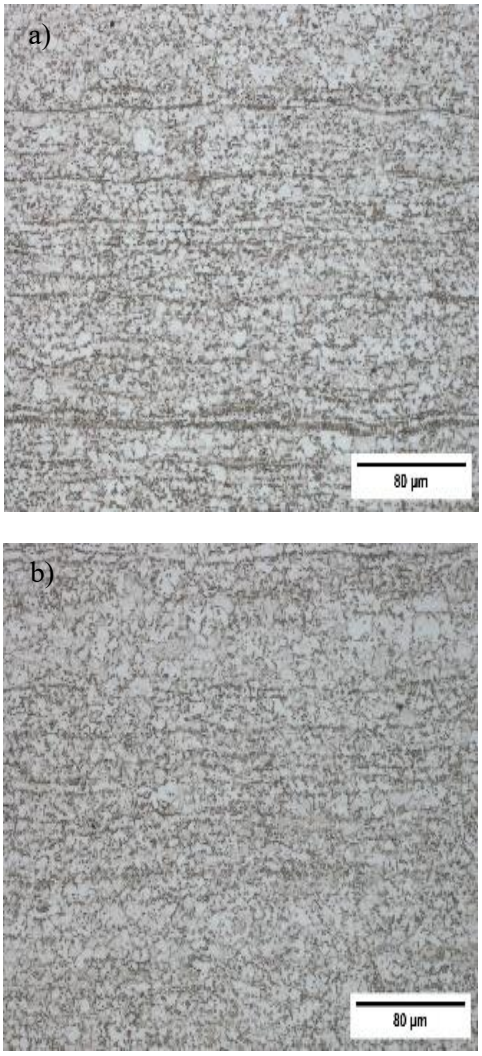

Figure 8. Optical microscope images a) EU1, b) EU2

Figure 9 shows the SEM microstructures of 600DU steel from distinct manufacturers at varying magnifications. The martensitic band structure in EU1 steel is clearly visible. Research indicates that increasing chromium, molybdenum, and niobium content results in a more ordered ferritic phase with clearer phase boundaries. Higher concentrations of chromium-enriched MA (martensite-austenite) islands within ferrite grains enhance austenite stability. Experimental steels with increased microalloying content concentrations improved elongation, reduced yield strength to tensile strength ratio, and better formability [29]. Additionally, Figure 9b and Figure 9c show that EU2 steel has a finer grain size than EU1 steel due to differences in production processes.

Celal Bayar University Journal of Science
Volume 21, Issue 3, 2025, p 10-20
Doi: 10.18466/cbayarfbe.1614992

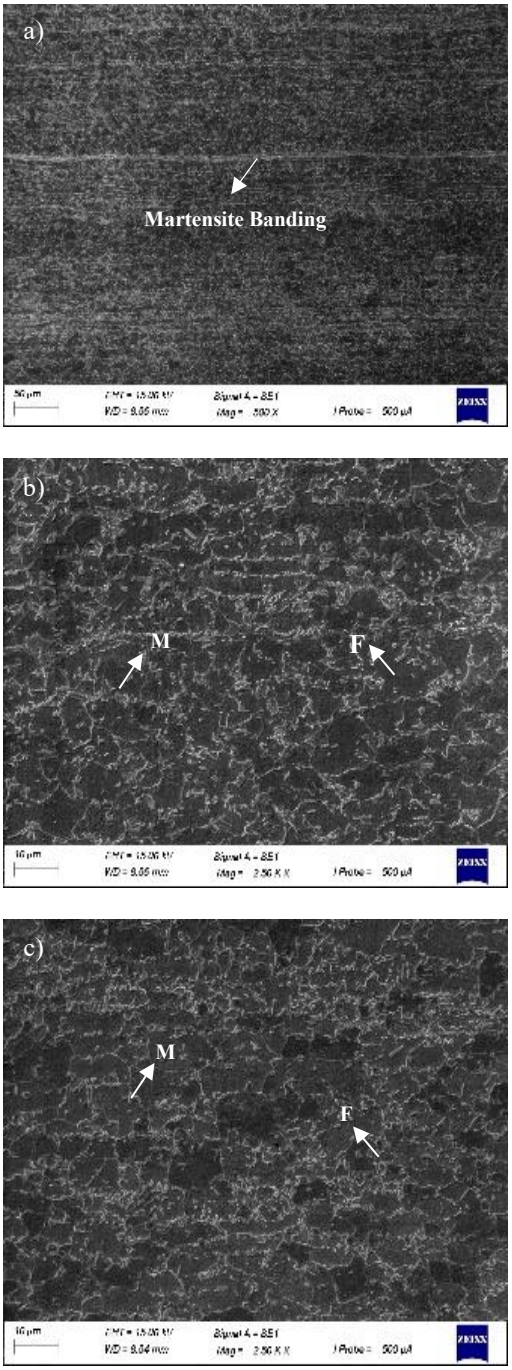

Figure 9. 600DU SEM images from different manufacturers a) low magnification EU1, b) high magnification EU1 and c) EU2

3.2. Mechanical Properties

Figure 10 illustrates stress-strain (%) graphs depending on different rolling directions of EU1 and EU2 steels. Both materials exhibited similar tensile strength values. Nonetheless, some difference between yield and elongation values is noticeable. Firstly, the directional percent elongation values are irregular in material EU1. This is due to the martensitic band structure found in the microstructure. The research found that cracks began forming in martensite regions, no matter what the overall structure looked like. It was observed that the presence of banded structure or equiaxed shaped martensite islands influenced how much the material could stretch before fracture. During tensile testing, the local strain measured at the point where failure started was 0.085 for the equiaxed microstructure and 0.06 for the banded microstructure [28, 30].

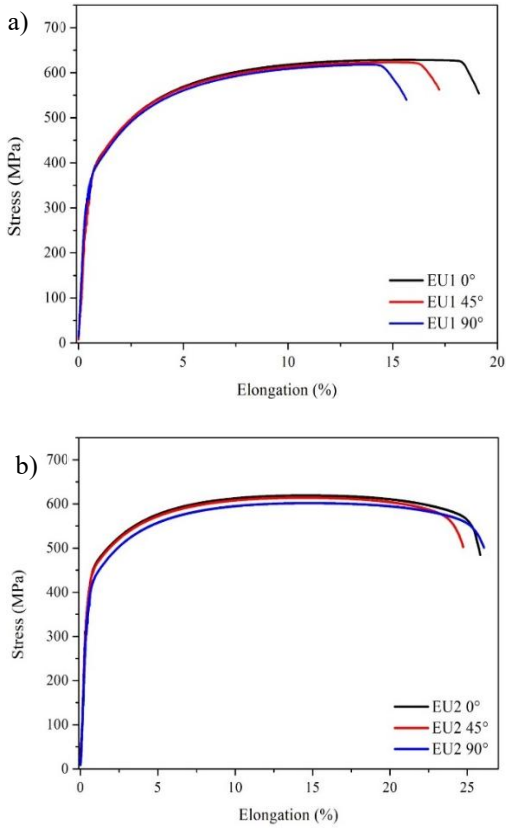

Figure 10. Tensile stress-strain curves of a) EU1 b) EU2

Table 2. Stress-strain values of different rolling directions of EU1and EU2 material

EU1	**(Rp0.2) MPa**	**Elongation (%)**	**(Rm) MPa**
0°	368.16	24.17	632.87
45°	353.10	21.65	626.86
90°	334.73	20.69	617.93
EU2	**(Rp0.2) MPa**	**Elongation (%)**	**(Rm) MPa**
0°	410.24	25.95	619.13
45°	405.59	25.66	608.82
90°	383.49	26.29	601.89

Furthermore, yield strength obeying the Hall-Petch relationship increases with decreasing grain size [31]. This decrease in grain size affects the hardness outcomes presented in Table 3 [32].

Table 3. Average hardness values of EU1 and EU2 materials

Specimen Code	**HV**
EU1	178
EU2	212

3.3 Hole Expansion Examination

The martensite microstructure in EU2 steel is no longer predominantly aligned along grain boundaries in a network or chain-like arrangement, instead EU1 exhibits a more dispersed pattern with many martensite band structures. As seen in Figure 11, the hole expansion test ceases at the observation of a crack through the thickness or when a load drop surpassing the designated value occurs, followed by subsequent measurements. The crack mechanism occurs in the martensite phase for DU steels under deformation. Damage occurs by crack nucleation and propagation. Crack propagation can be mitigated down by a number of effects. The enhancement of grain size has garnered interest in recent years. The reduction in grain size increases the distance necessary for crack propagation, therefrom elevating the energy demand for crack formation and damage [32]. EU2 steel command a more refined grain structure than EU1 steel and lacks equiaxed martensite banding. As seen in Figure 12, the average hole expansion ratios for EU1 and EU2 steels are 26.65% and 60.71% respectively, demonstrating a significant improvement in the formability of the latter. The research conducted supports this situation [31-33]. The anomalous fracture and elongation values observed in the tensile test results are also noticeable in the Hole Expansion results.

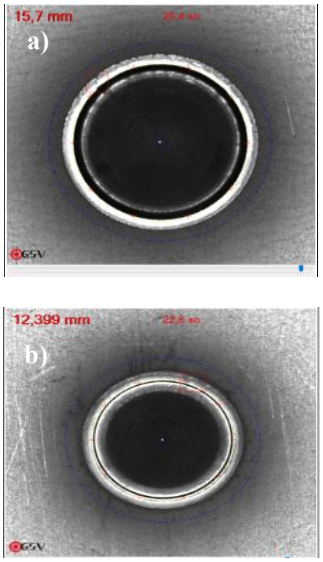

Figure 11. Camera images of the hole expansion test for specimens from different coil manufacturers a) EU2 b) EU1

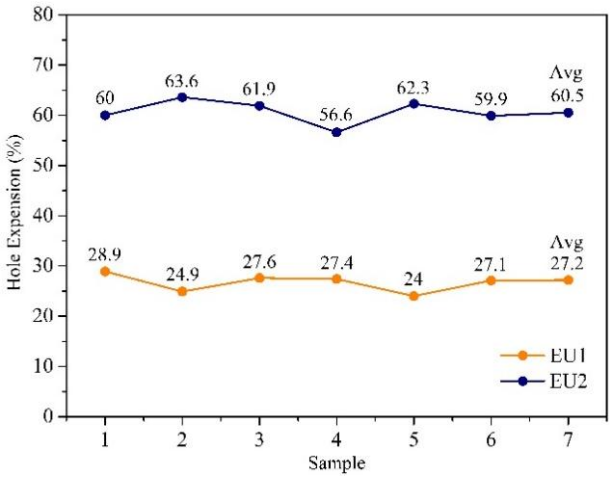

Figure 12. Comparison of hole expansion ratio values

3.4 Forming Simulation Analysis

As illustrated in Figures 13, the simulation results for 600DU-grade steels from EU1 and EU2 manufacturers were analyzed using the AutoForm application. The simulations utilized their respective material cards, and the results were evaluated based on the FLD (forming limit diagram) derived from the hardening and yield forming limit curves. Following the completion of the simulations, As illustrated in Figure 13, it was observed that at the two corner regions of the component, the thinning in EU1 material was 8% greater compared to EU2 material. As a result, higher levels of minor strain were recorded at the same corner points in the EU1 material, indicating a greater localized deformation in these regions.

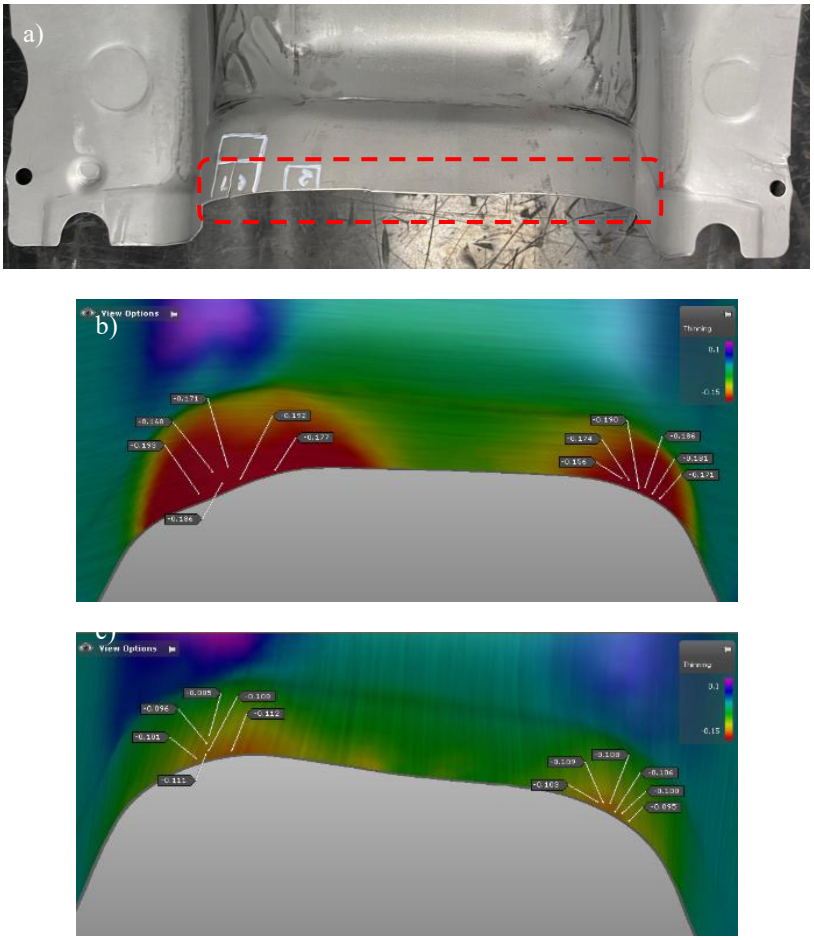

Figure 13. Images of AutoForm Simulation a) macro view of parts b) Thickness Results for EU1 Steel c) Thickness Results for EU2 Steel

3.5 Die Trials Results

The analysis of material behavior in cold forming processes is crucial for ensuring the quality of the final product and optimizing production efficiency. This study investigates the sheared edge quality, formability, and deformation characteristics of EU1 and EU2 materials, sourced from different steel manufacturers, by conducting trials using a press machine and a designated die. Prior to the experiments, factors that could potentially influence the process were meticulously evaluated. To assess the suitability of critical die components, a comprehensive inspection was carried out, including blank holders, scrap cutters, pilot pins, and pad plates, along with the overall condition of the die surfaces. No anomalies or irregularities were detected. After each press stroke, process panels were examined for burr formation, scrap indentation, and edge cracking, with particular attention given to deformations along the sheared edges. Additionally, during forming and bending operations, the formability and deformation behavior of the materials were closely monitored. The experimental findings indicate that the EU2 material exhibits superior sheared edge quality compared to EU1. While edge cracking was observed in EU1, no such defects were detected in EU2. Furthermore, thickness measurements were conducted using a strain gauge, and thickness reduction was calculated based on Equation 4. The results revealed that the final part produced from EU1 experienced an 18% reduction in thickness, whereas the

EU2-based part exhibited only an 11% reduction. Thickness reduction is directly related to the homogeneity of stress distribution during forming. The greater thinning observed in EU1 suggests lower toughness and a less uniform deformation response. These differences can be attributed to variations in the microstructural properties of the materials, particularly grain size and phase distribution. The finer grain structure and more homogeneous phase distribution of EU2 contribute to its higher mechanical strength and ductility, enhancing its resistance to edge cracking during forming operations [34]. These findings underscore the critical role of material selection in cold forming processes, directly impacting both production efficiency and the overall quality of the final product.

$$\text{Thickness} = \frac{\text{measured thickness}}{\text{nominal thickness}} - 1 \quad (4)$$

4. Discussion and Conclusion

In this investigation examines the prevalent issues of edge cracking and splitting encountered during cold forming of components fabricated from the same grade DU steels produced by various manufacturers. Within the scope of the investigation, factors affecting the formability of the materials were examined.

1. The simulation results revealed that at two specific regions, the thinning in EU1 material was found to be 8% higher compared to EU2 material. Additionally, the higher minor strains observed in EU1 at the same locations contributed to an increased amount of thinning in these regions. The consistency between the thinning percentages obtained from the simulation and those from the physical experiments demonstrates the reliability of the data. The martensitic band structure in the microstructure of EU1 material, due to its hardened nature, resulted in higher internal stresses, which led to thinning and subsequent edge crack formation in EU1 material.

2. The microstructural analysis indicates that the observed martensite band structure has a detrimental effect on the formability of the material. The hardness and heterogeneous nature of the martensitic regions can lead to an uneven distribution of deformation during forming processes. This results in increased resistance to processes such as tensile and bending operations, and the development of higher localized stresses. Consequently, these microstructural characteristics can make the material more prone to cracking and fracture, particularly during cold forming processes. This, in turn, can negatively impact the efficiency and safety of the material during the manufacturing process.

3. The steel samples, labeled EU1 and EU2, with distinct grain size structures, were evaluated based on mechanical test results. The finer-grained microstructure of the EU2 steel, as demonstrated by the Hall-Petch relationship, can potentially increase the yield strength, elongation, and hardness values This increase is primarily attributed to the accumulation of dislocations along the grain boundaries, which enhances the hardness of the material. In general, grain refinement is associated with an increase in hardness and yield strength, but it is also correlated with a decrease in ductility. However, material failure involves crack initiation and subsequent crack propagation. With a reduction in grain size, the distance required for crack propagation increases, which can make crack advancement more challenging. This effect may enhance the crack resistance of the material, thus helping to prevent edge cracking and splitting during forming. These findings were corroborated by Hole Expansion tests. Despite its finer-grained microstructure, EU2 material demonstrated superior formability compared to EU1 material. A more definitive conclusion can be obtained by establishing a crack penetration map and conducting a detailed analysis.

4. It was observed that the thinning values obtained during the trial were very close to the measured thinning values. This suggests that the simulation results, based on the material cards selected for EU1 and EU2 materials, align with the experimental outcomes. This observation supports the accuracy and reliability of the simulation.

In investigation, this study demonstrates that the mechanical properties of DU steels can be optimized through microstructural modifications, potentially reducing issues encountered during production. These findings hold practical application potential for steel manufacturers and industries such as automotive, which utilize DU steels. During the trials conducted under die and press synchronization, tests performed using 600DU steel revealed edge cracking in the material sourced from the EU1 steel producer, while no such defects were observed in the material supplied by the EU2 steel producer. These observations were corroborated through microstructural examinations and mechanical testing, with the obtained results aligning with the observed discrepancies. Dual Phase (DP) materials exhibit distinct characteristic properties that differentiate them from conventional steels. The differing mechanical behavior of the hard and ductile phases leads to the emergence of

unique fracture mechanisms, primarily governed by void nucleation and coalescence processes. Studies have demonstrated that while a material may fulfill all the mechanical requirements of Dual Phase steels, it may fail to meet the minimum local formability parameters, particularly edge stretchability. These discrepancies are primarily attributed to factors such as microstructural homogeneity (grain size) and inclusion content, both of which are directly associated with the steelmaker's quality grade. In this context, the findings of the present study align with these observations in the literature, further supporting the influence of microstructural characteristics on local formability capacity [20]. Furthermore, the findings indicate that the microstructural and mechanical properties of the steels from the two producers differ, and these variations can directly affect the material performance. Additionally, future studies could investigate the effects of different mechanical tests, such as fracture toughness and dynamic strain aging, on the process performance of DP steels.

Acknowledgement

TOYOTETSU Türkiye provided support for the production and analysis of the materials used in this study.

Author's Contributions

Zeki Ahmet Ekmen: Drafted and wrote the manuscript, performed simulation result analysis.

Yiğit Gönülalan: Assisted with laboratory tests.

Onur Muratal: Provided support in interpreting the measurement and test results.

Diğdem Atabek: Help with writing the experimental test results.

Ethics

There are no ethical issues after the publication of this manuscript.

References

[1] Mutafi, A., Yidris, N., Koloor, S.S.R., Petrů, M. Numerical Prediction of Residual Stresses Distribution in Thin-Walled Press-Braked Stainless Steel Sections, 13(2020), 5378.

[2] Hu, Xiaohua., and Feng, Zhili ,2021, Advanced High-Strength Steel - Basics and Applications in the Automotive Industry, United States.

[3] Nanda T., Singh V., Singh V., Chakraborty A, Sharma S. Third generation of advanced high-strength steels: Processing routes and properties, 233(2019), 209-238.

[4] Galán, J., Samek, L., Verleysen, P., Verbeken, K., & Houbaert, Y. (2012). Advanced high strength steels for automotive industry 48(2012), 118-131.

[5] Cui H, Li D, Fu Q, Lu Z, Xu J, Jiang N. Research on Forming Limit Stress Diagram of Advanced High Strength Dual-Phase Steel Sheets. Materials 16(2023),4543.

[6] Jean-Hubert Schmitt , Thierry Iung. New developments of advanced high-strength steels for automotive applications, 19(2018), 641-656.

[7] Yuntian Zhu, Xiaolei Wu. Heterostructured materials, 131(2023), 101019.

[8] WorldAutoSteels Advanced High-Strength Steels Application Guidelines Version 6.0, https://www.worldautosteel.org/download_files/AHSS%20Guidelines%20V6/00_AHSSGuidelines_V6_20170430.pdf (Access date: April 2017)

[9] Saai, A., Hopperstad, O.S., Fritz, J. et al. A numerical study on the effects of DU steel microstructure on the yield locus and the stress–strain response under strain path change, 16(2023)

[10] Taamjeed Rahmaan, 2015. Low to High Strain Rate Characterization of DP600, TRIP780, AA5182-OM. Department of Mechanical and Mechatronics Engineering the University of Waterloo, Master of Science Thesıs, 147s. Waterloo.

[11] Tısza M. Development of Advanced High Strength Automotive Steels, 4(2021), 9-17.

[12] Merve Çobanoğlu, 2019. Damage ın Dual Phase Steels Under Industrıal Formıng Condıtıons. School of natural and applıed scıences of Middle East Technical University, Master of Science Thesıs, 140, Ankara.

[13] Hall, J., Coryell, J., Wendt, B., and Adamski, D. Case Studies of Edge Fracture of Dual Phase Steel Stampings, 8(2015), 783-788.

[14] Hulka, Klaus. Modern Multi-Phase Steels for the Automotive Industry, 414–415(2003), 101–110.

[15] Berkay Bayramin, 2017. Dynamıc Straın Agıng of Dual Phase Steels ın Formıng Applıcatıons Mıddle East Technıcal Unıversıty, Natural and Applıed Scıences Master of Science Thesıs, 85, Ankara.

[16] Habibi, N., Mathi, S., Beier, T., Könemann, M. Münstermann, S. Effects of Microstructural Properties on Damage Evolution and Edge Crack Sensitivity of DP1000 Steels,12(2022), 845.

[17] M, R., S.K., Schmidova, E., Konopík, P., Melzer, D., Bozkurt, F., V Londe, N. Fracture Toughness Analysis of Automotive-Grade Dual-Phase Steel Using Essential Work of Fracture (EWF) Method, 10(2020), 1019.

[18] Zinan Li, Yuling Chang, Wenqi Liu, Junhe Lian. Predicting edge fracture in dual-phase steels: Significance of anisotropy-induced localization, 274(2024), 109255.

[19] Xin Wua, Hamed Bahmanpour , Ken Schmid. Characterization of Mechanically Sheared Edges of Dual Phase Steels 212(2012), 1209-1224.

[20] Carlos R.M.Silva, F.J.G Silva. Investigations on the edge crack defect in Dual Phase steel stamping process, 17(2018), 737-745.

[21] Habibi, N., Beier, T., Richter, H., Könemann, M., & Münstermann, S2019. The effects of shear affected zone on edge crack sensitivity in dual-phase steels. In IOP Conference Series: Materials Science and Engineering (Vol. 651, November, 012073. Netherlands.

[22] Khalilabad, M.M., Perdahcıoğlu, S., Atzema. Initiation and growth of edge cracks after shear cutting of dual-phase steel, 127(2023), 2327–2341.

[23] Peter Sachnik, Sheikh Enamul Hoque, Wolfram Volk. Burr-free cutting edges by notch-shear cutting, 249 (2017), 229-245.

[24] Nasheralahkami, S., Zhou, W., and Golovashchenko, S. Study of sheared edge formability of ultra-high strength DP980 sheet metal blanks, 141(2019), 091009.

[25] Vukota Boljanovic. 2004. Sheet Metal Forming Process And Die Design, America, 230s.

[26] Bassini, E.; Sivo, A.; Ugues, D. Assessment of the Hardening Behavior and Tensile Properties of a Cold-Rolled Bainitic–Ferritic Steel, 14(2021), 6662.

[27] Graux, A.; Cazottes, S.; Castro, D.D.; San-Martín, D.; Capdevila, C.; Cabrera, J.M.; Molas, S.; Schreiber, S.; Mirković, D.; Danoix, F. Design and Development of Complex Phase Steels with Improved Combination of Strength and Stretch-Flangeability, 10(2020), 824.

[28] Pütz, F., Shen, F., Könemann, M. The differences of damage initiation and accumulation of DP steels: a numerical and experimental analysis, 226(2020), 1–15.

[29] Yun, H. A. N., Kuang, S., Liu, H. S., Jiang, Y. H., & Liu, G. H. Effect of Chromium on Microstructure and Mechanical Properties of Cold Rolled Hot-dip Galvanizing DP450 Steel, 22(2015), 1055–1061.

[30] A. Ramazani, Z. Ebrahimi, U. Prahl, Study the effect of martensite banding on the failure initiation in dual-phase steel,Computational Materials Science, 87(2014), 241-247.

[31] Chen X, Liang J, Yang D, Hu Z, Xu X, Gu X, Xie G. Effect of Chromium on Microstructure and Mechanical Properties of Hot-Dip Galvanized Dual-Phase (DP980) Steel, 13(2023), 1287.

[32] Meyers, M. A., & Chawla, K. K. 2008. Mechanical behavior of materials. Cambridge University Press.

[33] Ji Hoon Kim, M.G. Lee, D. Kim, D.K. Matlock, R.H. Wagoner. Hole-expansion formability of dual-phase steels using representative volume element approach with boundary-smoothing technique, 527(2010), 7353-7363.

[34] Queiroz, R. R. U., Cunha, F. G. G., & Gonzalez, B. M. Study of dynamic strain aging in dual phase steel. Materials Science and Engineering: A, 543(2012), 84-87.